SOCAR

SOCAR Proceedings

Geology, Geophysics & Formation Evaluation

journal home page: http://proceedings.socar.az

A NEW APPROACH TO DETERMINE THE BEST ESTIMATE OF WATER SATURATION

N. Sh. Aliyev[1], G. I. Jalalov[2], E. N. Alizade[3]

[1]*«OilGasScientificResearchProject» Institute, SOCAR, Baku, Azerbaijan*

[2]*The Azerbaijan National Academy of Sciences, Baku, Azerbaijan*

[3]*BP Azerbaijan, Baku, Azerbaijan*

A B S T R A C T

The research demonstrates that an explicit probabilistic approach can estimate the most probable porosity solution within the uncertainty range of porosity logging tools. By iteratively adjusting estimated volumes and fluid saturations to minimize the difference between theoretical and measured log responses, the approach provides a more robust interpretation than conventional deterministic methods. Although some resolution may be reduced in low-porosity or thin-bedded intervals, integrating multiple log responses and applying statistical minimization reduces sensitivity to individual parameter uncertainties, such as an incorrect saturation exponent. The results also provide a basis for evaluating logging-tool confidence and assessing the reliability of porosity and water-saturation estimates. The research further demonstrates that forward modeling can be used to simulate the effects of mineralogy, flushed-zone saturation (Sxo), invasion diameter, hydrocarbon correction magnitude, and end-member responses on nuclear logging measurements. This modeling approach supports quality assurance of log data and facilitates the evaluation of alternative lithological scenarios prior to detailed petrophysical analysis. The GCA-1 well in the Chirag field was selected as the key well for this study due to its comprehensive dataset, which includes full log suites, core analysis, pressure transient analysis, and repeat formation testing. The workflow involves conducting a robust log analysis on GCA-1, identifying the least common denominator (LCD) log set shared with other wells in the field and applying an LCD-based model across the broader well population. This ensures consistent and reliable petrophysical interpretation. A modified version of Wyllie-Rose empirical equation adequately predicts the core-measured permeability. The modified equation uses porosity and initial water saturation as regression parameters. The combination of initial water saturation techniques and Leverett J function could be useful after waterflood or aquifer encroachment. Finally, a new empirical method was developed to quantitatively predict the log-derived saturation profile using a non-Archie-based solution. This method minimizes the sum of squared differences between measured mercury capillary pressure data and theoretical values based on a proposed equation. It demonstrates excellent agreement with the porosity, saturation, and permeabilities derived from different approaches described in the article, highlighting the effectiveness of this integrated approach for comprehensive reservoir evaluation.

Keywords: water saturation; log analysis; capillary pressure; cementation and saturation exponents; NMOD; permeability; invasion; net mean stress.

Date submitted: 03.08.2026 **Date accepted:** 11.09.2026

© 2026 «OilGasScientificResearchProject» Institute. All rights reserved.

Introduction

Explicit probabilistic method [1-7] gives the most probable porosity solution within the uncertainty range determined for the porosity logging devices. The method uses an interim guess of solution volumes including lithology (V_{litho}), shale volume (V_{sh}), porosity (φ), and fluid saturations to compute the corresponding theoretical log responses, which are then compared to the actual measurements. A minimization algorithm iteratively adjusts these volumes and saturations to reduce the error between modeled and recorded log responses.

While some resolution may be lost in low-porosity zones or thin-bedded formations, explicit probabilistic method offers a more robust interpretation than deterministic methods. Unlike deterministic approaches – which can yield incorrect water saturation values if the saturation exponent is misestimated - probabilistic method is less sensitive to individual parameter errors. It uses multiple log responses and statistical minimization, which helps to reduce the influence of single-variable inaccuracies. Additionally, it computes uncertainties in the output results, enabling risk-weighted evaluation of porosity and water saturation.

The GCA-1 well was selected as the key well for this study due to its comprehensive dataset, including a full suite

*E-mail: nusret.aliyev@socar.az

http://dx.doi.org/10.5510/OGP20260301226

of logs, core data, pressure transient analysis (PTA), and repeat formation testing (RFT) [8]. The workflow applied to the Chirag field is as follows: a) perform a detailed log analysis on the GCA-1 key well, b) identify the least common denominator (LCD) log set shared between GCA-1 and other wells in the field, c) build a model based on GCA-1 that best replicates the robust interpretation using the LCD logs and d) apply the LCD-based model to the remaining wells in the Chirag field to ensure consistency and reliability across the petrophysical interpretations.

A modified version of the Wyllie-Rose empirical equation [9, 10] adequately predicts the core-measured permeability. The modified equation uses porosity and initial water saturation (S_{wi}) as regression parameters (not applicable if initial water saturation is altered due to waterflooding or aquifer encroachment). The combination of S_{wi} techniques and Leverett J may be useful after waterflood or aquifer encroachment. The modified Leverett J method [2, 11] is an excellent procedure for predicting log-determined water saturation data from high-pressure mercury capillary pressure measurements.

A new empirical method is developed that allows quantitative prediction of a log saturation profile using a non-Archie solution. It minimizes the sum of the square difference between the measured and theoretical (based on a proposed equation) mercury capillary pressure data. This method is applied and results in excellent prediction of log saturation data.

Methods applied

The petrophysical integration process model (PIPM). PIPM [12] was applied to evaluate formation evaluation (FE). Major components of the FE applied are

1. Log analysis to determine pore volume and hydrocarbon saturation
2. Core permeability prediction by calibrating logs to core-measured data
3. Verification, estimation of water saturation using non-Archie-based solutions
4. Verification of the Free Water Level (FWL) from capillary pressure responses and comparing it to the RFT analysis

Log analysis. The primary objective of quantitative log analysis is to determine values for a variety of primary parameters, such as porosity (reservoir storage capability), shale volume saturation (the hydrocarbon type and content) and permeability (reservoir productivity).

Secondary aspects, such as composition of lithic volume and well-to-well correlation (mapping reservoir parameters), can be derived by integrating outputs obtained from quantitative log analysis, steps 1-3.

Assuming data is environmentally corrected, there are two main classes of quantitative log analysis techniques:

- Deterministic analysis, which assumes a relating log measurements to reservoir lithology, pore system characteristics, and fluid content, with each log measurement used independently.
- Explicit probabilistic analysis, on the other hand, is performed using routines such as OPTIMA™, ULTRA™ and GLOBAL™. A compositional model of the formation is assumed (lithology and hydrocarbon system), and explicit equations are applied to describe each log response to the components as a homogeneous mixture. Shale volume, porosity and water saturation are calculated explicitly by minimizing the error between theoretical and recorded responses (e.g., gamma ray, resistivity, density, neutron, etc.).

Both deterministic and probabilistic techniques are utilized in this study to analyze the GCA-1 data. PowerLog™ software was used for deterministic log analysis and OPTIMA™ in combination with NMOD for probabilistic log analysis. NMOD is used to quality check log responses and to calculate the end-member nuclear tool response for shale and sand.

In OPTIMA™, log responses are reconstructed by adjusting variables such as pore volume, fluid composition, invasion profile, and mineralogy, all under the constraint that the total volume, comprising porosity and matrix components, sums to unity.

In this study, for robust log analysis of the GCA-1 well, mineral parameters were determined using NMOD. The input logs used include gamma ray, neutron, density, deep resistivity, micro resistivity, and sonic.

In the Chirag field, the reservoir fluid is oil at its bubble point, meaning that saturation effects on porosity logs are relatively minor. In contrast, gas reservoirs would require significantly more rigorous corrections due to the greater influence of gas on neutron and density log responses.

Analysis and results

This study focuses on the GCA-1 well, located in the Chirag field. Although many wells have been drilled in the field, GCA-1 is the only one with a complete dataset, including a full suite of logs, core data, pressure transient analysis (PTA), and RFT (Repeat Formation Tester) data. [8, 13]

The following step-by-step procedure was used to perform the quantitative log analysis for GCA-1 well:

1. Apply environmental corrections, accounting for factors such as mud invasion, formation temperature, brine salinity, borehole washouts, etc.

2. Depth-align the core data to match the log depth reference, including gamma ray, porosity, and permeability measurements.

3. Correct core-measured porosity and permeability to net mean stress (NMS) conditions to represent in-situ values.

A robust GCA-1 log interpretation requires iterative application of the following steps (4–6), using resistivity, sonic, density, and gamma ray logs, until a satisfactory match with core-measured porosity is achieved. Due to its poor quality, the photoelectric factor (*Pe*) log was excluded from the analysis. To improve the match accuracy, the Pereriv and Balakhany intervals were subdivided into four subintervals.

4. Determine shale and sand end-member properties using NMOD modeling.

5. Estimate the cementation exponent (m), saturation exponent (n), and formation water resistivity (R_w) from electrical log data.

6. Predict porosity, water saturation, and volume of shale using OPTIMA™.

Once a satisfactory match with the core-measured porosity was achieved, the following steps (7 and 8) were carried out to complete the analysis:

7. Predict core permeability using the Kipling method

and a modified Wyllie-Rose empirical correlation, based on porosity and water saturation.

8. Determine water saturation and free water level (FWL) using the capillary pressure data n combination with log-determined porosity and permeability. During this step, the consistency of water saturation endpoints (S_{wi}) obtained from relative permeability and capillary pressure tests was also verified.

Before proceeding to Step 9, the least common denominator (LCD) of available logs between the GCA-1 key well and other wells in the Chirag field was identified. Based on this shared set of logs, a representative LCD model was developed to replicate the results of the robust GCA-1 log analysis. This model was then applied to the other wells using NMOD and OPTIMA™ techniques (Steps 4–8).

9. Perform log analysis (predict porosity, permeability and water saturation) for additional logs using trained models derived from the GCA-1 log analysis.

As noted earlier, the following logs were used in the GCA-1 analysis: gamma ray, gamma ray spectral, dual lateral resistivity, sonic, density, and compensated neutron. The photoelectric (*Pe*) log was excluded due to poor data quality.

From the GCA-1 and A1–A8 wells in the Chirag field, characteristic «fingerprints» or response patterns of these logging tools were observed.

Gamma ray. Gamma ray logs are used for formation correlation and bed boundary determination, evaluation of the shale content of a formation, mineral analysis and perforating depth control and tracing of radioactive fluid movement. Since gamma rays can pass through the steel casing, measurements can be performed in both open and cased holes. Gamma rays originate from three main sources in nature: the radioactive elements in the uranium group, the thorium group, and potassium. Gamma ray logs are subject to a number of perturbing effects, including position in the hole (centered/eccentered), hole size, mud weight, casing size and weight and cement thickness.

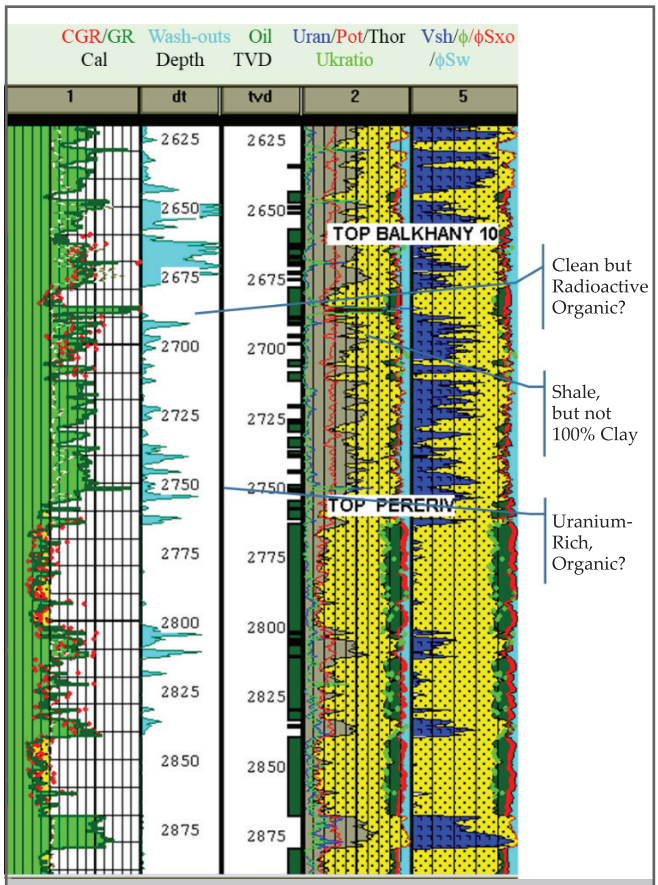

Fig. 1. Gamma ray, spectral gamma ray for the GCA-1 well

Gamma ray spectral log. The ratio of thorium to uranium varies depending on the depositional environment; it is typically highest in continental oxidizing settings and lower in marine environments. The uranium to potassium ratio has been found to correlate well with potential source rock in argillaceous sediments. Additionally, the thorium-to-potassium ratio has proven effective in distinguishing between different types of clay minerals, as noted in the Schlumberger Log Analysis Manual [14].

Figure 1 presents both the gamma ray and spectral gamma ray logs for the GCA-1 well. The spectral gamma ray (the concentration curves of uranium, thorium and potassium) has several potential applications, including the way formation is deposited (deltaic, channel or lacustrine), what has happened to the formation since its deposition, a mechanism for tracing the interwell continuity across the field (correlation to depositional environment, diagenetic process, clay type, and clay volume), and most importantly, the estimation of shale content.

Dual laterolog (DLL). Laterologs are usually used when there is seawater or brine mud in the hole, the R_{mf}/R_w ratio is less than about 3 and the hole size is less than 16 inches. This tool makes two resistivity measurements: the laterolog deep (LLd) and the laterolog shallow (LLs). A microresistivity log may be run in conjunction with the laterolog measurements. Under the normal conditions found when using a dual laterolog, the radial profile of resistivities is $R_t > R_{xo} > R_m$. Between the invaded zone and the undisturbed formation is a transition zone with a resistivity value between R_t andR_{xo}.

The microresistivity log is useful for determining S_{xo}, residual oil saturation, hydrocarbon movability (permeability), hydrocarbon density, and invasion diameter. The water (filtrate) saturation in the flushed zone (S_{xo}) can be calculated by the Archie equation. The invasion process of filtrate acts like a miniature waterflood; it displaces both connate water and movable hydrocarbons. In its undisturbed state, at initial reservoir conditions, the fractional pore volume occupied by hydrocarbon is $\phi(1 - S_w)$. After filtrate invasion, the fractional pore volume occupied by hydrocarbon is $\phi(1\text{-}S_{xo})$. The difference between these two values is the fractional pore volume that contains movable oil $\phi(S_{xo} - S_w)$. The fraction of the original oil in place that has moved is determined by:

$$\frac{\varnothing\left(S_{xo} - S_w\right)}{\varnothing\left(1 - S_w\right)} \text{ or } \frac{\left(S_{xo} - S_w\right)}{\left(1 - S_w\right)}$$

This ratio is a measure of the quality of the pay. In formations where permeability to oil (relative permeability in more than one-phase flow) is low, S_{xo} is likely to be close to S_w, and the ratio will be low.

Figure 2 shows two logs. The log on the top is the GCA-1 well log and as expected there is a significant separation between R_{LLd} and R_{MLL} indicating an oil zone. Note that R_{LLd} has much higher value than the RMLL. On the other hand, the log on the bottom is the A-4 well log; this well was drilled in water leg. The R_{MLL} log has a bit higher value than both R_{LLd} and R_{LLs}, but overall there is almost no separation between all three resistivity logs.

Environmental correction. Gamma ray, dual laterlog resistivity and compensated neutron logs are environmentally corrected for mud invasion, temperature, salinity, and washouts. As shown in figure 3, there is about 2.5-12 % correction in gamma ray response. This tool has the largest environmental correction compared to all the other tools.

Large corrections are needed in depths corresponding to a high degree of washouts

Lab data depth shift. Comparison of the log-predicted porosity, permeability and water saturation to lab-measured data requires depth-shifting the core data. Common practice is to cross correlate the core and log gamma rays and then use the shift table to depth shift porosity and permeability. Figure 4 shows a comparison of the depth shifted core gamma ray to the log gamma ray; the calculated correlation coefficient is in excess of 0.73, which indicates logs are in good agreement.

Porosity and permeability net mean stress correction. The net mean stress or confining pressure, acting on a rock, increases as reservoir pressure depletes during the primary production of the Chirag reservoir. Three separate NMS analyses of the Chirag field log data indicate values in the range of 4300-5700 psi. A minifrac test result, which was conducted in the productive sands in the GCA-1 well. A minimum closure stress ratio of 0.91 (minimum horizontal stress divided by vertical stress) was calculated based on this test. Three triaxial geomechanical tests conducted at confining pressures of 502, 1203 and 2503 psi using GCA-1 core plugs. The GCA-1 log data including dipole sonic.

Nigel Higgs [15, 16] conducted a burial history and depletion modeling of the Chirag field using the latest triaxial data and minifrac-determined stress ratio of 0.91 with the StressPATH one-dimensional elasticity-based simulator. He estimated the NMS to be about 5400 psi (in order to match the 0.91 ratio, the model was subjected to a 1% horizontal strain in one of the horizontal directions). In a parallel study, Martin Traugott [17, 18], using the same information and the GCA-1 log data, assuming plate tectonics, calculated a NMS of 4300 psi (NMS=3000 psi without plate tectonics). He suggested running core plug electric measurements using a vertical effective stress of 4300 psi. Furthermore, Kent Newsham [19] using GCA-1 dipole sonic logs, determined the NMS of a 4700-5700 psi range. Both dynamic and static determination is used in the geomechanical models.

These values are significantly above the NMS value of 2600 psi used by R.Sigal in previous work. According to Ted Braun [11], the value of 2600 psi was determined from an existing correlation using geomechanical-input parameters (Young and Bulk moduli) from an analogue offshore reservoir to perform the calculation. Ted also commented that this value is rather optimistic.

Porosity and permeability as a function of NMS were examined over a range of 400-3700 psi by AZLAB and a range of 400-2600 psi by PTS Lab. The measurements also made in the range of 400-6000 psi. According to the legacy data, an average 5-8% (1-2 P.U. – porosity unit) reduction in porosity and 12% in permeability are reasonable for a NMS increase from 400 psi to 4500 psi (see fig. 5). Measured core porosities and permeabilities at 400 psi are corrected for stress effect and used throughout this study. The NMS in this field is expected to increase initially until planned water injection is commenced, at which point the NMS will stay the same or close to the original value.

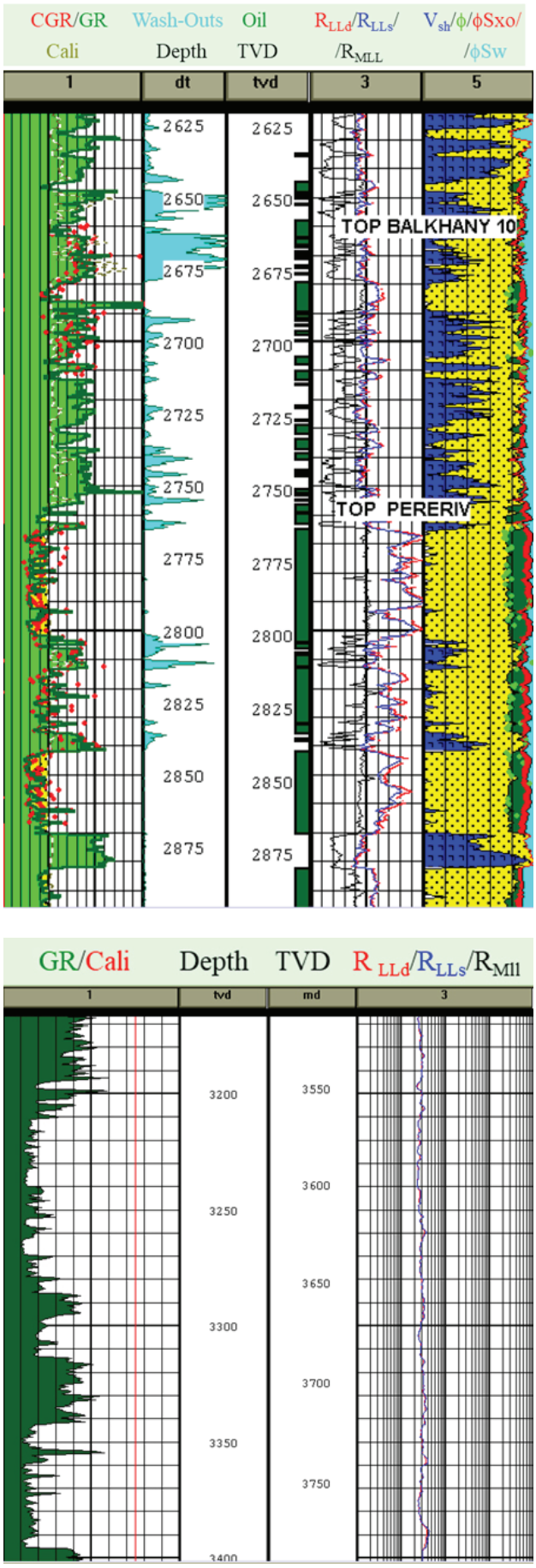

Fig. 2. Comparing resistivity logs for GCA-l and A-4 wells in the Chirag field

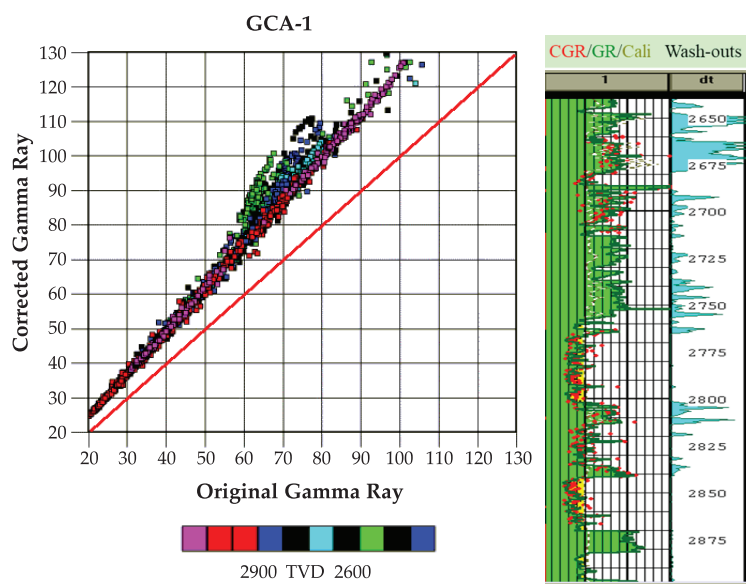

Fig. 3. Gamma ray environmental correction

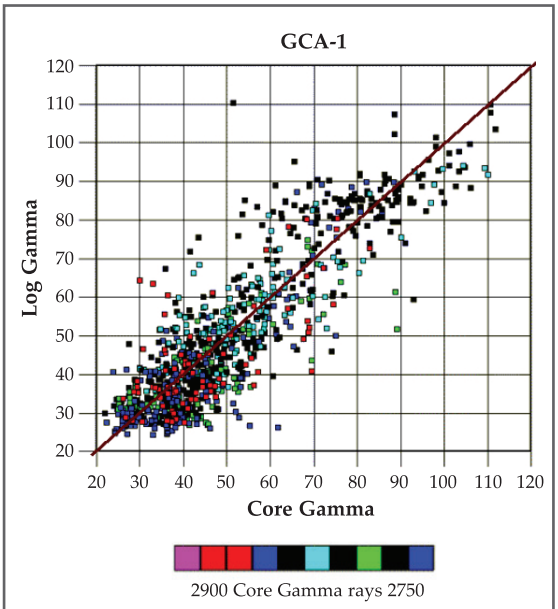

Fig. 4. Comparison of depth-shifted core and log Gamma rays

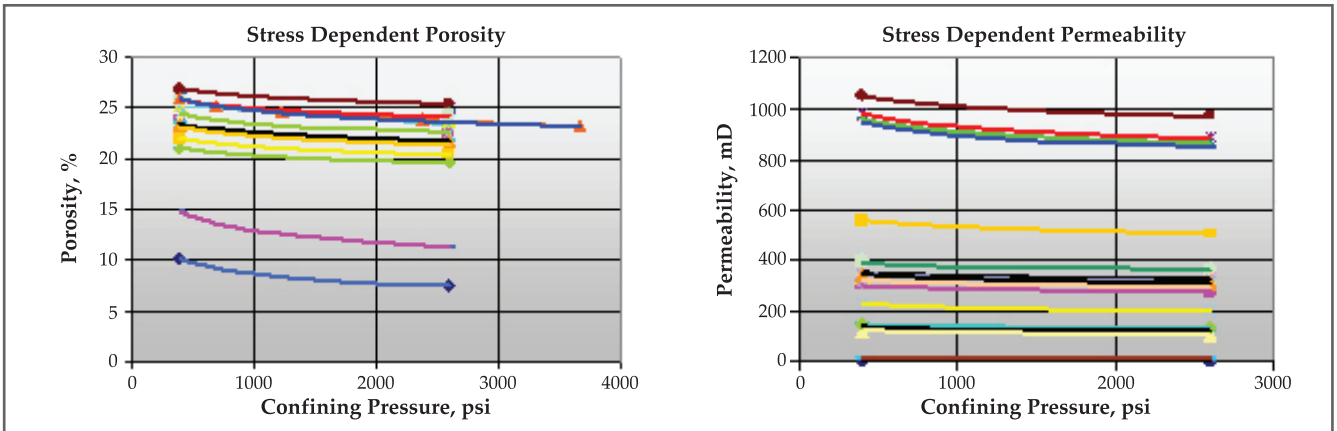

Fig. 5. Stress dependency of porosity and permeability for core plugs from the GCA-1 well

End-member determination. Shale and sand end members are determined by cross plotting log responses using NMOD. The NMOD-modeled mineral points are then input into OPTIMA™ or PowerLog™ to perform log analysis.

Electrical property measurements. One of the main objectives of this study is to determine the correct Archie's saturation exponent (n). The previous data from two independent labs show values ranging from 1.4 (using cold extract for cleaning core slow flow for displacement) to 1.8 (using the hot extract technique to clean the cores). The saturation exponent is a critical parameter which directly impacts the oil-in-place calculations.

A novel experimental core analysis procedure was proposed to determine electrical properties and capillary pressures using samples representing different rock types.

1. *Tests 1A*-3A*:* Fresh-state electrical resistivity and capillary measurements at the reservoir temperature of 145° F and a confining pressure of 4500 psi.

2. *Tests 1A-3A:* Fresh-state electrical resistivity and capillary measurements at ambient temperature of 77° F and a confining pressure of 4500 psi (vacuum dried at 140° F).

3. *Tests 1B-3B:* Cold solvent cleaned for electrical resistivity and capillary pressure tests at 77° F and 4500 psi confining pressure (vacuum dried at 140° F).

4. *Tests 1C-3C:* Flow through cleaned for electrical and capillary pressure measurements at 77° F and 4500 psi confining pressure (no pre-test drying).

5. *Tests 1D-3D:* Hot solvent cleaning technique for electrical and capillary pressure measurements at 7 ° F and 4500 psi confining pressure (vacuum dried at 140° F).

Water resistivity (R_w). Connate waters range in resistivity from 01 of an ohm-m up to several ohm-m, depending on the total dissolved solids concentration (salinity or TDS) and temperature of the formation water. A value of R_w is required to determine water saturation by the quantitative log analysis.

A synthetic water composition (19000 ppm sodium chloride, 500 ppm calcium chloride and 500 ppm potassium chloride) is used to represent the formation water in all electrical property measurement tests. A value of 0.1676 ohm-m is measured at the reservoir confining pressure of 4500 psi and the temperature of 145° F.

Cementation and saturation exponents (m and n). Laboratory measured data (PTS Lab, 1999) shows that there is

no trend versus the ($\sqrt{\kappa}/\%\phi$) and relatively small variations in measured cementation (m) and saturation (n) exponents. Average values of 1.84 and 1.64, for n and m respectively, are used for the GCA-1 log analysis. Since there is no trend in «n» and «m» with rock types, it is not necessary to perform Waxman-Smits type calculations.

Pickett plot for the Pereriv interval using the average m and n values and the measured R_w value of 0.1675 ohm-m (reported by PTS Lab).

Porosity determination. As stated earlier, both deterministic and probabilistic methods are used to predict volume of shale and porosity. The Shaly Sand model in PowerLog™ is used for deterministic calculations, and a combination of OPTIMA™ and NMOD is used for probabilistic estimations. A comparison of log and core porosity profiles is shown in figure 6. The deterministic method underestimates the core porosity, whereas the probabilistically determined porosity profile agrees fairly well with core-measured values [20, 21].

The deterministic profile underestimates porosity at high values whereas the probabilistic profile is in good agreement with the core measured data. Figure 7 indicates a good correlation between predicted and measured porosity profiles (correlation coefficients >0.8). Since the log-calculated porosity profile is often used in predicting the permeability, an accurate log-predicted porosity profile is extremely important.

Permeability prediction. While porosity is a static property of a rock, permeability is a dynamic one. Permeability is a measure of the ability of a rock to allow fluids to flow through it. Therefore, accurate prediction of permeability is essential for an accurate forecast of reservoir performance (rate and recovery). Two mathematical approaches are used to predict core permeability data:

Kipling™ implicit probabilistic method – Unlike the explicit techniques, which use equations to define the basic relationships of the measurements, the implicit routines use correlation to infer the relationships between the data. The Kipling™ method can be used for either non-parametric regression or non-parametric discriminant analysis, developing a model for the prediction of either a continuous variable (such as permeability) or a categorical variable (such as lithofacies) based on a set of underlying predictor variables (a set of well logs, for example) [22]. The shale volume (V_{sh}), log-predicted porosity (ϕ) and log-predicted water saturation (S_w) are used as estimators of permeability.

A Modified Version of the Wyllie-Rose Empirical Expression [9, 10] – The following equation is used:

$$k = 50000 \times (\phi^5) / (Sw^{0.9})$$

This equation does fairly well predicting permeability above 10 mD. Figures 8-10 show the comparison of log and core permeability profiles for the Pereriv interval of the GCA-1 well [13]. This technique requires Swi. However, as the field matures and waterflooding is introduced, a recalibration will be required. Also, no core exists in the aquifer. Further study of the aquifer is necessary for adequate characterization.

Good agreement between the modified Wyllie-Rose and core-measured profiles. Since k is a strong function of ϕ, it is critical to predict core-measured ϕ accurately.

Water saturation prediction. So far a fairly good match of core porosity and permeability data were obtained. The final piece of the puzzle is to verify log-determined water saturation using capillary pressure data and compare the predicted free-water level from high-pressure mercury injection capillary pressure data versus field-determined value. In this study two non-Archie saturation models were employed to predict the GCA-1 log calculated water saturation profile:

1. Modified Leverett J method using representative capillary pressure curves for different rock types [23].
2. The new saturation model developed in this study.

Modified Leverett J saturation model. The classic Leveret J function [24] defines the relationship between the porosity-permeability ratio (k/ϕ) and the water saturation at a given height above the free water level (FWL):

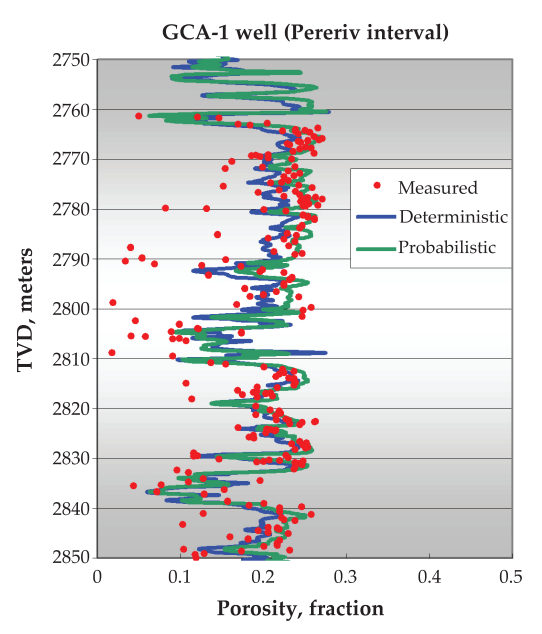

Fig. 6. Comparison of log-calculated and core-measured porosity data

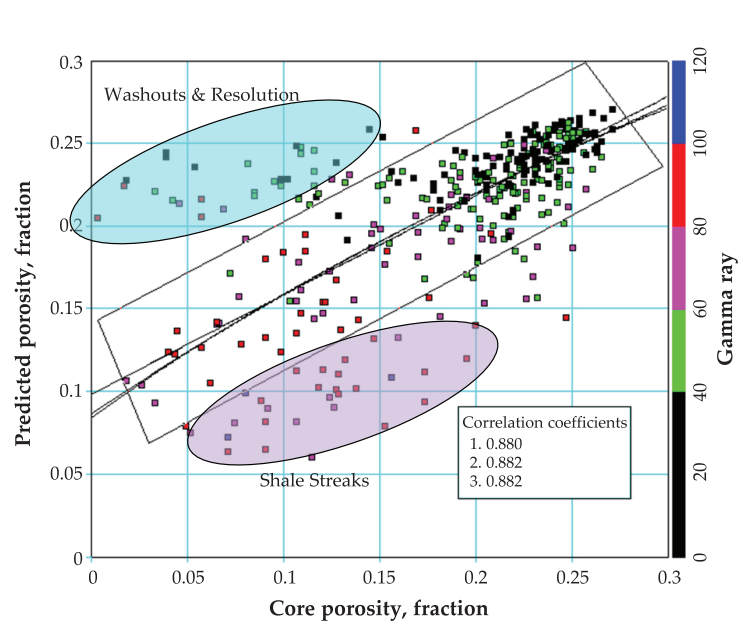

Fig. 7. Good correlation coefficient between log-and core-measured porosity data

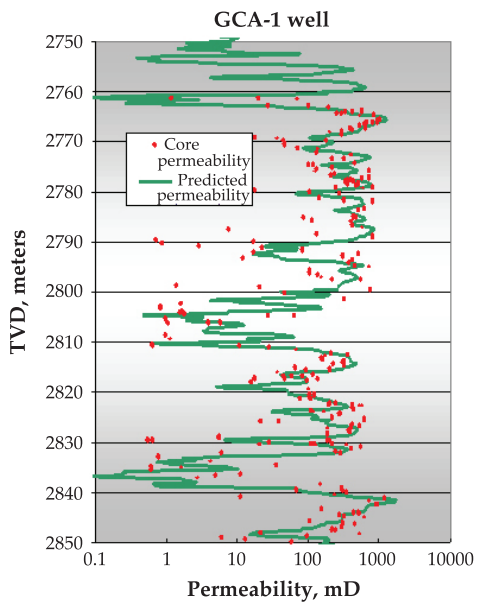

Fig. 8. Comparison of log-calculated and core-measured permeability profiles

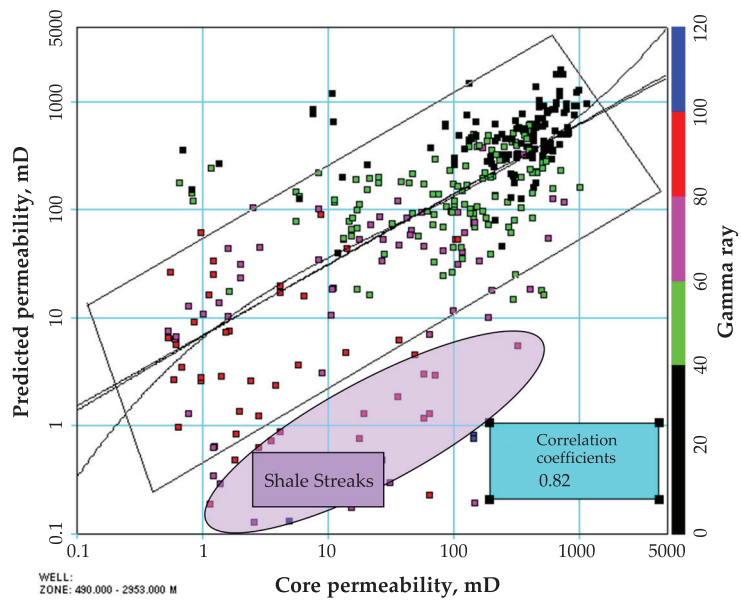

Fig. 10. Good correlation coefficient between log-and core-measured permeability profiles

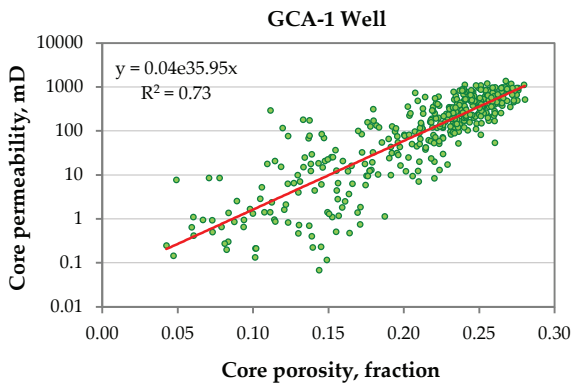

Fig. 9. Correlation coefficient between the log-predicted and core-measured permeability data

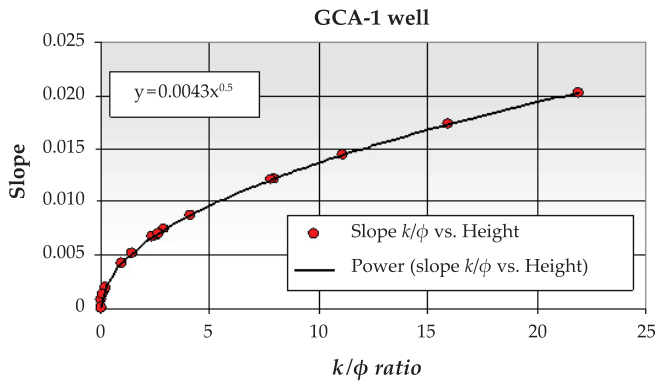

Fig. 11. Slope J to height vs k/ϕ ratio

$$J(Sw) = \frac{0.391 \cdot Pc}{2T\cos\vartheta}\sqrt{\frac{k}{\phi}}$$

where $J(Sw)$ is the Leveret J function; Pc is the capillary pressure in psi; T is interfacial tension in dynes/cm; ϑ is the contact angle in degrees; k is the permeability in mD; and ϕ is the porosity in percent.

The procedure for predicting log water saturation profile is given by Gunter et al. [23]. The procedure includes following steps:

1. Transform initial rock data into petrophysical rock types.
2. Convert capillary data into height above free water level.
3. Compute Leverett J function.
4. Establish the graphical relationship of the Leverett J vs. height above the FWL.
5. Find the following relationship

$$Slope\ J\ \ vs\ H = C \cdot \left(\frac{k}{\phi}\right)^{0.5}$$

6. Use representative capillary pressure curves for each rock type to predict water saturation using log-determined k/ϕ ratio.

The k/ϕ ratio is an excellent mechanism for independently discriminating rock types. This fundamental property has proven to be a guide for unlocking complex pore geometry. It also provides a linkage to forms of more continuous data sources such as wireline and LWD.

Our extension to the classical Leverett technique is to compute the coefficient of a power fit to the plot of the slope of J versus height above free water level as a function of k/ϕ ratio (fig. 11).

The Pereriv and Balakhany X reservoirs have separate oil-water contacts and are modeled independently. The predicted J-function water saturation profile matches the log-derived water saturations well in the Pereriv interval (dominated by rock types 1- 4). On the other hand, in the Balakhany X interval, which is dominated by rock types 3-6, the match is not as good. Figure 12 shows the comparison between predicted modified Leverett J and the log-calculated water saturation profiles. The calculated FWL of 3050 meters is in good agreement with the RFT-determined value of 3100 meters.

A good comparison of capillary-pressure-predicted water saturation to log interpretation was obtained. The modified Leverett J theory collapses capillary pressure curves by rock type to predict water saturation. The predicted FWL of 3050 meter is in close agreement with RFT-determined value of 3100 meters (AIOC reported a value in the range of 3075-3100 meters).

A new saturation model. In this study, a newly developed mathematical expression predicts the capillary pressure from the non-wetting saturation:

$$Pc = a \times \mathrm{EXP}(b \times Sw) \times Sw^{c}$$

where *Pc* is the capillary pressure in psi; *Sw* is the water saturation; and *a*, *b* and *c* are model constants. These constants are determined by regression of the measured capillary pressure data. Figure 13 depicts very good matches of a few selected measured capillary pressure data using the new equation.

Obtained excellent matches to measured capillary pressure data using the new mathematical model.

To generalize the correlation for predicting capillary pressure across all rock types, the variable $\sqrt{\kappa/\phi}$, representing the controlling rock type speed, was employed. Three points from each curve were then selected:

1. Water saturation (*Sw*) at 2000 psi which represents the end point water saturation,

2. *Sw* and *Pc* at the apex (the inflection point on the capillary pressure curve). The apex point is the maximum on the plot of (100-Sw)/Pc versus (100-Sw). For more details on the apex method, read Pittman [25] and Swanson [26].

3. *Pc* values at 95% *Sw* (entry point on the capillary pressure curve).

Excellent power fit to data (correlation coefficients > 0.95 for all cases).

Figure 14 shows excellent correlation between the measured variables and the common variable $\sqrt{\kappa/\phi}$, with power regression correlation coefficients exceeding 0.95 for all four data sets. Based on these power functions, a family of capillary pressure curves was generated and applied in water saturation predictions. Figure 15 presents the resulting family of capillary pressure curves produced using this method.

Finally, as shown in figure 16, the capillary pressure-predicted water saturation profile shows excellent agreement with the log-determined saturation profile in the Pereriv interval and good agreement in the Balakhany X interval. The predicted free water level (FWL) of 3100 meters matches the RFT-determined value. A Microsoft Excel worksheet has been developed to perform all calculations automatically, with the FWL value as the only adjustable parameter.

The capillary-pressure-predicted water saturation profile is in excellent agreement with the log-determined saturation profile for the Pereriv interval. Also, the predicted FWL of 3100 is the same as the RFT-determined value of 3100 meter.

The user must be aware of the following pros and cons regarding the new model:

- ϕ and *k* must be of high quality.
- Best applicable to unimodal capillary pressure curves.
- Best applicable to capillary pressure data which do not cross each other.
- Best applicable if measured data are sampled from all rock types.
- Must have porosity and permeability associated with each sample used to measure capillary pressure. This is needed to determine power functions used to define model constants as a function of $\sqrt{\kappa/\phi}$.

Since the new model uses three data points from the capillary pressure curve to determine model constants, it does not require continuous capillary pressure data. Therefore, one can use either porous plate or high pressure mercury injection data.

The method was used to extrapolate the GCA-1 well capillary pressure data to predict the log saturation profiles for several nearby wells and obtained excellent matches.

Finally, the consistency of the capillary pressure and

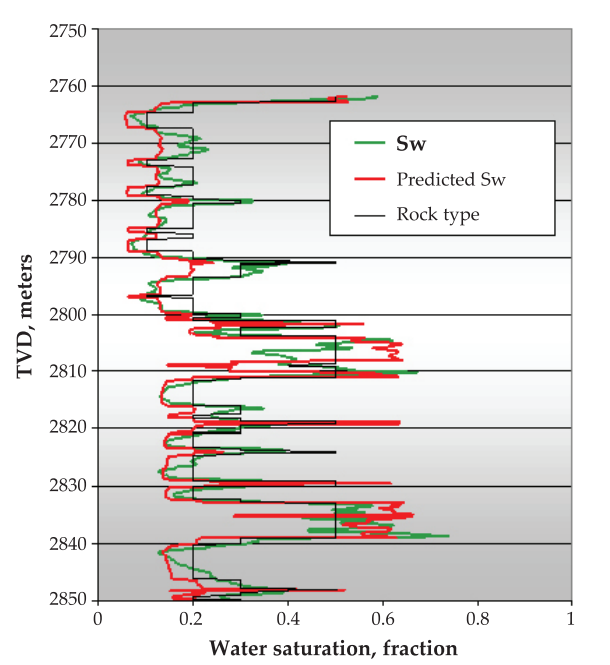

Fig. 12. Modified Leverett J vs log-calculated water saturation profiles

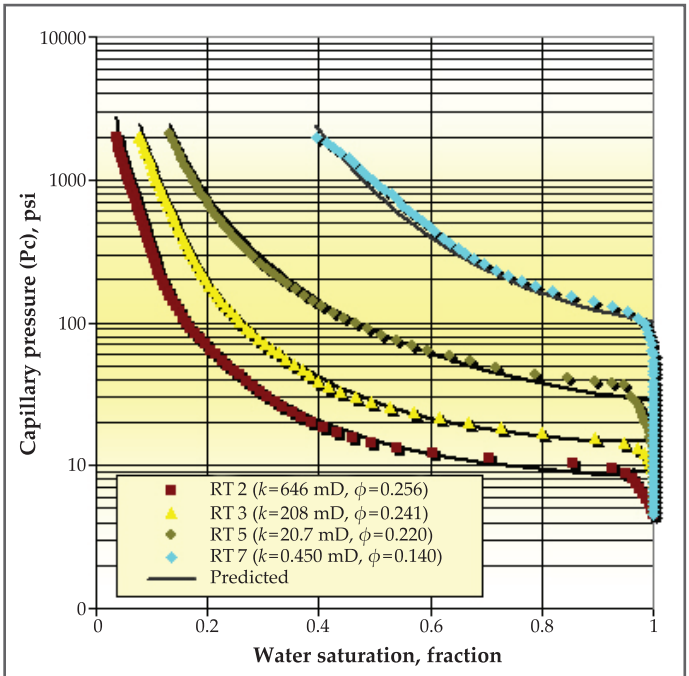

Fig. 13. Comparison of the predicted and measured capillary pressure curves

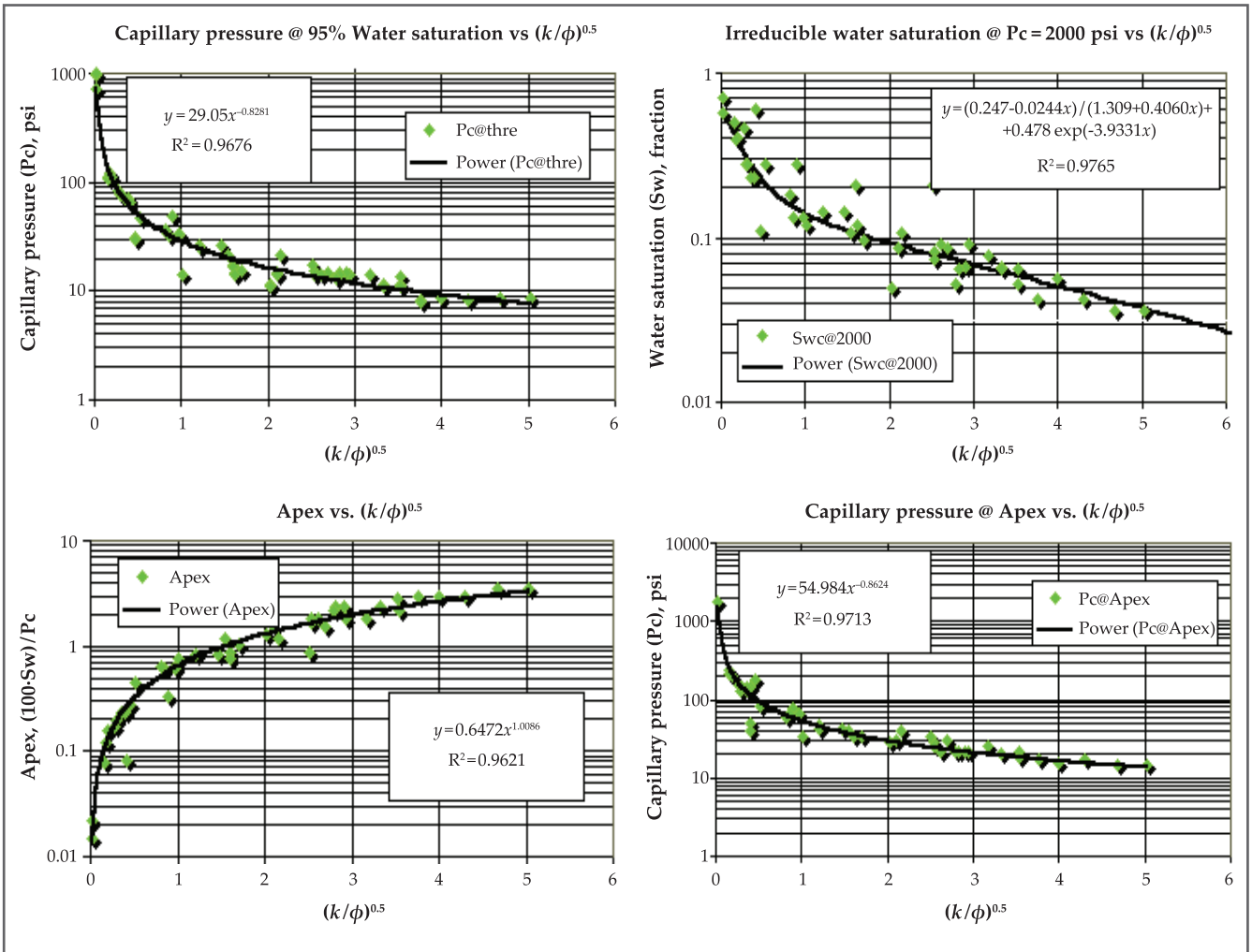

Fig. 14. Plots of variables vs $\sqrt{k/\phi}$

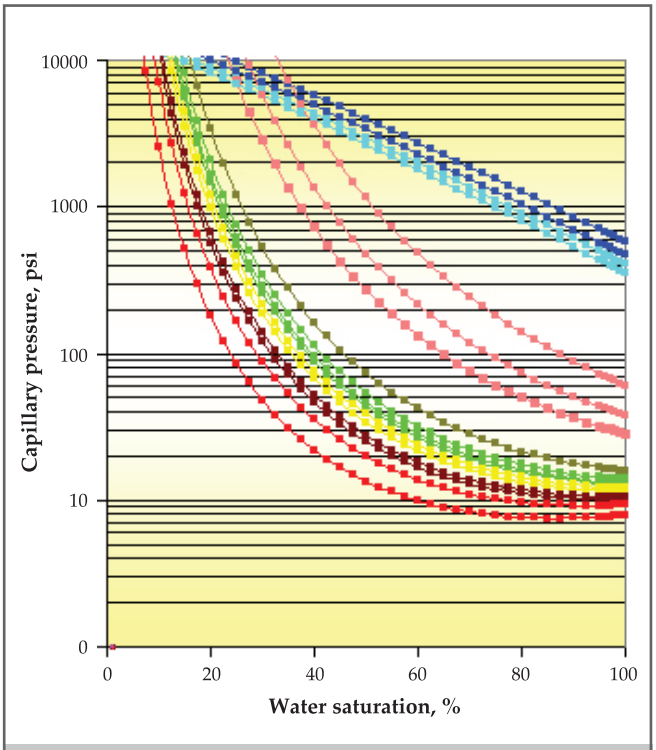

Fig. 15. Generated capillary pressure curves for the GCA-1 well using the new model

relative permeability data is examined. Permeability is first correlated as a function of porosity and end-point water saturation (*Sw* at 2000 psi) for the capillary pressure data, using a function similar to that applied in log analysis (the modified Wyllie-Rose equation). Predicted permeability is then plotted based on porosity and end-point water saturation using the same equation. The predicted permeability from relative permeability tests, derived using the capillary pressure correlation, shows good agreement with the measured data, with a correlation coefficient of approximately 0.90.

Final log results. The lithofacies and rock type predictions use the Kipling method. Overall, predicted and observed data agree well. The pay is estimated by including porosity greater than 8% (on the third track, shaded dark-green). Red symbols represent core data and lines are log analysis results.

Log analysis is performed using both explicit and implicit probabilistic analysis routines after core data is depth-shifted and corrected for environmental effects. The OPTIMA™ software is used to explicitly determine shale volume, porosity, and water saturation profiles by minimizing the error between theoretical and log-recorded responses (Gamma Ray, Resistivity, Density, Neutron, etc.). A modified version of the Wyllie and Rose correlation ($5000 \times \phi^5 \times Swi^{0.9}$) is then applied to predict permeability. The 'KIPLING' method is used to implicitly predict lithofacies and rock types

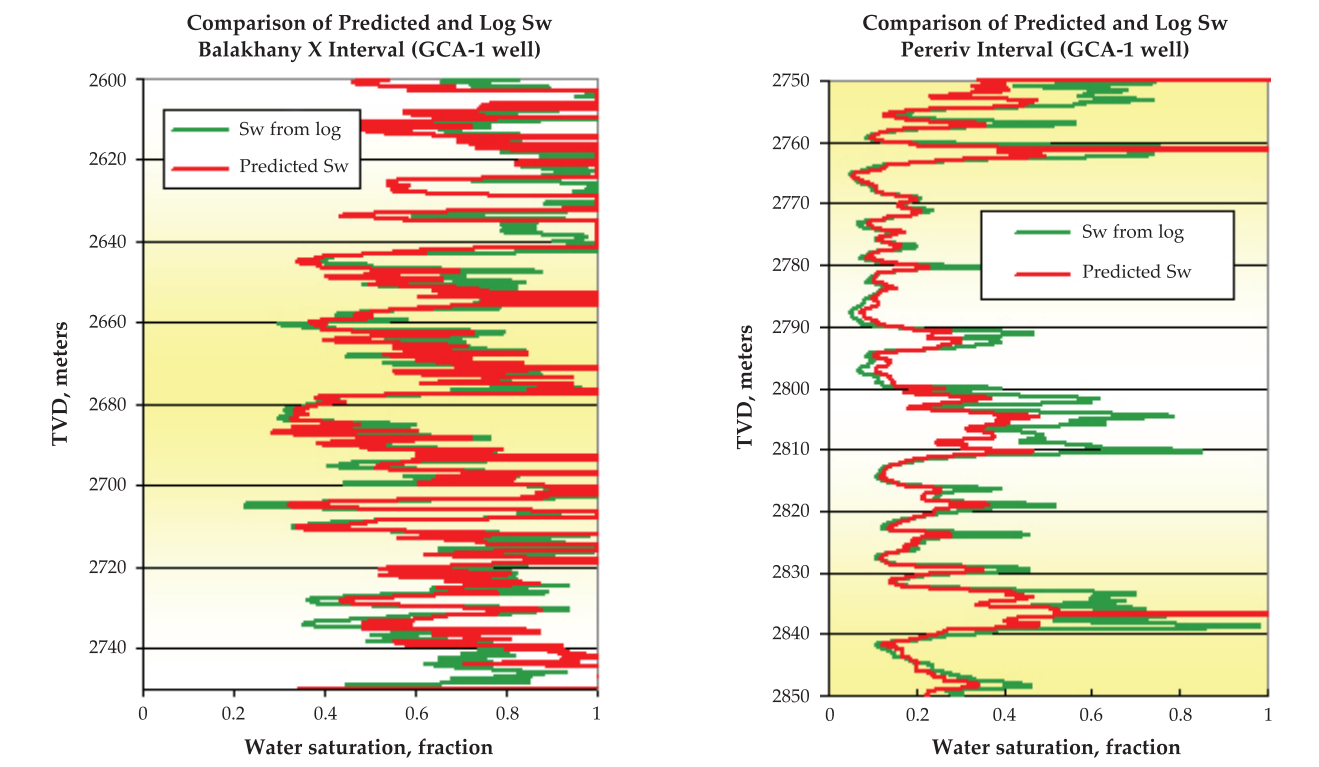

Fig. 16. The new saturation model capillary pressure vs log-calculated water saturation profiles

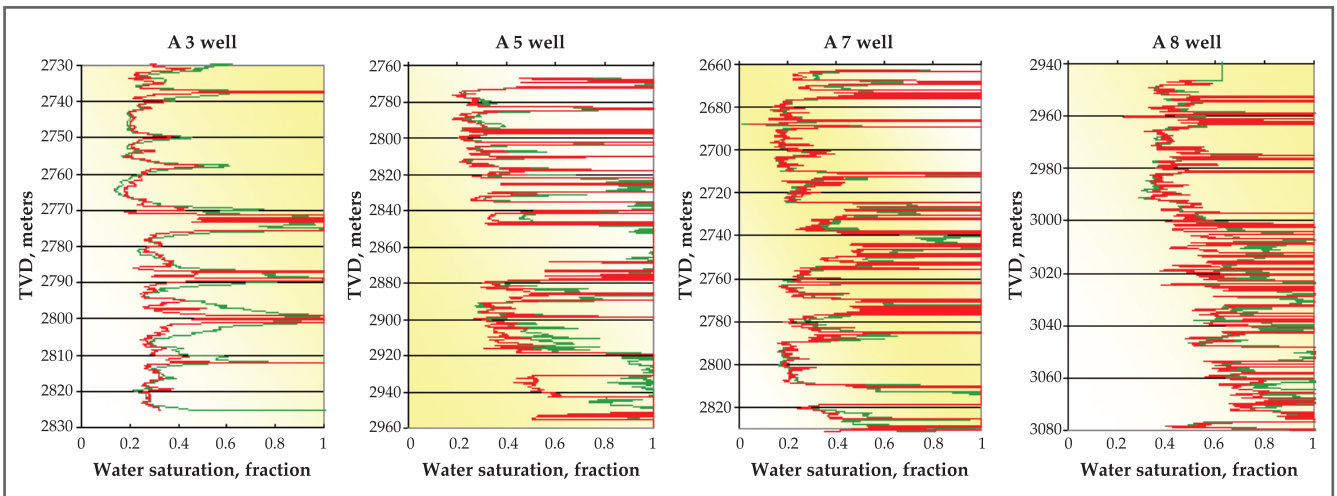

Fig. 17. Predicted Water Saturation Profiles vs Log Calculated Values

through correlations inferred from relationships among the log data. This approach enables to obtain a good match with laboratory-measured core porosity and permeability data. Additionally, the predicted water saturation from capillary pressure data shows very good agreement with the log-derived water saturation profile.

Log analysis for additional wells. Log analysis is performed on four A3, A5, A7 and A8 close-by wells using OPTIMA™ and NMOD techniques using the least common denominator of log tools which are common among all these wells and the GCA-1 well. After estimation of porosity and water saturation, a modified Wyllie-Rose correlation is used to predict the permeability profile.

Using the new saturation model and the GCA-1 well capillary pressure data log water saturation profiles and FWLs were predicted. As shown below in figure 17, predicted water saturation profiles are in good agreement with log-determined profiles for all wells (A-3, A-5, A-7 and A-8). This indicates that the method proposed can successfully scale properties from the GCA-1 well measured core and log data to other wells in the Chirag field.

Good extrapolation from the GCA-1 well data to other nearby wells using the newly developed saturation model, OPTIMA™ and NMOD.

Conclusions

The probabilistic approach delivers the most probable porosity and saturation values within tool uncertainty limits. It minimizes error between theoretical and measured logs, producing more robust and reliable results than deterministic methods. It also calculates uncertainty in outputs, enabling risk-weighted decisions.

NMOD forward models the effects of mineralogy, invasion diameter, and hydrocarbon correction, ensuring log data quality and supporting lithologic scenario planning.

GCA-1 was used as the reference well due to its comprehensive dataset. A robust model built from GCA-1 logs was calibrated to other wells using a least common denominator (LCD) log set, enabling consistent analysis across the Chirag field.

A modified Wyllie-Rose equation, using porosity and initial water saturation (*Swi*), reliably predicts core-measured permeability, except in water-invaded zones. For post-flood conditions, Swi methods combined with Leverett J improve accuracy.

A modified Leverett J method effectively predicts water saturation from mercury capillary pressure data. A new empirical, non-Archie method further enhances log saturation predictions by minimizing differences between measured and theoretical capillary pressure, validated across multiple studies.

References

1. Hertzog, R., Colson, L., Seeman, B., et al. (1987). Geochemical logging with spectrometry tools. SPE-16792-PA. *SPE Formation Evaluation*, 4(02), 153-162.

2. Herron, M. M. (1987). Geochemical classification of terrigenous sands and shales from core or log data. *Geological Society of Sedimentary Petrology*, 58, 820-829.

3. Jackobson, L. A., Wyatt, D. F. (1996). Elemental yields and complex lithology analysis from the pulsed spectral gamma log. *The Log Analyst*, 37(01), 50-64.

4. Mezzatesta, A., Rodriguez, E., Fros,t E. (1988, 01 August). Optima: a statistical approach to well log analysis. *Geobyte*, 3(3), 56-69.

5. Rodriguez, E., Mezzatesta, A., Telzlaff, D. (1989, 13-15 December). Determination of statistical confidence interval for petrophysical formation properties. In: *SPWLA, LASER Symposium for Log Analysis Software and Review, London, England.*

6. Aliyev, N. Sh. (2024). Waterflood reservoir modelling for Chirag oilfield. *SOCAR Proceedings*, 1, 40–47.

7. Aliyev, N. Sh. (2025). Integrated upscaling techniques in Chirag reservoir modelling. *SOCAR Proceedings*, 4, 31–38.

8. Aliyev, N. Sh., Negahban, Sh. (2000). Petrophysical characterization and reservoir modeling of GSA fields. In: *AAPG Regional International Conference, July 9-12, Istanbul, Turkey.*

9. Wiley, R., Patchett, J. (1994, 19-20 June). The effects of invasion on density/thermal neutron porosity interpretation. In: *The SPWLA 35th Annual Logging Symposium, Tulsa, Oklahoma.*

10. Wyllie, M. R. J., Rose, W. D. (1950). Some theoretical considerations related to the quantitative evaluation of the physical characteristics of reservoir rock from electrical log data. SPE-950105-G. *SPE JPT*, 2(04), 105-118.

11. Braun, Ted. (2011). Some practical lessons learned during 30 years in the SCAL Lab. SCA2011-01. In: *The International Symposium of the Society of Core Analysts held in Austin, Texas, USA, 18-21 September.*

12. Gunter, G. W., Pinch, J. J., Finneran, J. M., Bryant, W. T. (1997). Overview of an integrated process model to develop petrophysical based reservoir descriptions. SPE-38748-MS. In: *The SPE Annual Technical Conference and Exhibition, San Antonio, Texas, October.*

13. Gunter, G. W., Sigal, R. F. (1997). Gunashli-Chirag-Azeri (GCA) GCA Well No. 1 Caspian Sea, Azerbaijan Core Study. July.

14. Schlumberger. (1989). Log interpretation principles and applications. *Houston: Schlumberger Wireline and Testing.*

15. Palmer, I., Higgs, N., Moschovidis, Z., Cameron, J. (2005, June). How 3D Stresses can change the standard thick-walled cylinder approach to sand prediction. In: *The Alaska Rocks 2005, The 40th U.S. Symposium on Rock Mechanics (USRMS), Anchorage, Alaska.*

16. Palmer, I., Ispas, I., Higgs, N., et al. (2002, 21-22 February). Stressman website to screen for potential geomechanical problems due to depletion. In: *International Symposium and Exhibition on Formation Damage Control, Lafayette, Louisiana.*

17. Tiab, D., Donaldson, E. C. (1996). Petrophysics. *Houston, TX: Gulf Publishing Company.*

18. Traugott, M. O. (1997). Pore / fracture pressure determination in deep water. *Deepwater Technology Supplement to World Oil*, August, 68-70.

19. Newsham, K. E., Rushing, J. A. (2001). An integrated work-flow model to characterize unconventional gas resources: Part I - Geological assessment and petrophysical evaluation. SPE-71351-MS. In: *The SPE Annual Technical Conference and Exhibition, New Orleans, Louisiana, September.*

20. Patchett, J., Wiley, R., El Bahr, M. (1993). Modeling the effects of glauconite on some openhole logs from the Lower Senonian in Egypt. SPWLA-1993-RR. In: *The SPWLA 34th Annual Logging Symposium, Calgary, Alberta, June.*

21. Patchett, J., Wiley, R. (1994). The effects of invasion on density/thermal neutron porosity interpretation. SPWLA-1994-G. In: *The SPWLA 35th Annual Logging Symposium, Tulsa, Oklahoma, June.*

22. Bohling, G. C., Doveton, J. H., Watney, W. L. (1996). Systematic identification of sequence stratigraphic units from wireline logs. In: *Stratigraphic analysis utilizing advanced geophysical, wireline and borehole technology for petroleum exploration and production. Presented at the Gulf Coast Section SEPM 17th Annual Research Conference.*

23. Gunter, G. W., Smart, C. R., Miller, M. A., Finneran, J. M. (1999). Saturation modeling at the well log scale using petrophysical rock types and a classic non-resistivity based method. SPWLA-1999-Z. In: *The SPWLA 40th Annual Logging Symposium, Oslo, Norway, May.*

24. Leverett, M. H. (1941). Capillary behavior in porous media. *AIME Petroleum Transaction*, 243, 149-156.

25. Pittman, E. D. (1992, February). Relationship of porosity and permeability to various parameters derived from mercury injection capillary pressure curves for sandstones. *AAPG Bulletin*, 76, 191-198.

26. Swanson, B. F. (1981). A simple correlation between permeabilities and mercury capillary pressure. *SPE JPT*, 33(12), 2498-2504.

27. Brain, G., Aliyev, N. (2012). Simulation modelling of Chirag field water cut. In: «*Khazarneftgazyatag– 2012» Scientific – Practical Conference, Baku, Azerbaijan.*

28. White, A. J., Traugott, M. O., Swarbrick, R. E. (2002). The use of leak-off tests as means of predicting minimum in-situ stress. *Petroleum Geoscience*, 8(2), 189-193.